On Constructing Globally Convergent Algorithms: Applications to GPR and Marine CSEM Sounding

A. Timonov
University of South Carolina Upstate, USA

Abstract— A new approach to constructing globally convergent algorithms for the approximate solution of some coefficient inverse problems arising in electromagnetic frequency sounding is presented. Utilizing the original transformations developed for the convexification method, this approach possesses two disctinctive features: (1) Bregman iterations, and 1) the refinement with the interior data. These novelties may significantly enhance both the spatial and contrast resolutions of quantitative imaging. These algorithms can be applied to quantitative imaging in GPR and marine CSEM sounding. Some results of computational experiments are presented.

1. INTRODUCTION

Marine CSEM sounding has been in commercial use for hydrocarbon exploration since the beginning of the 21st century, though it was first proposed in the 60s last century. In the last decade, marine CSEM sounding has become significant due to the growing interest to hydrocarbon deposits on a shelf, as well as to the rapid development of the efficient inversion techniques and technologies used in marine geophysics (see, e.g., [2]). The same is true for Ground Penetrating Radar (GPR) field whose diversity of applications includes geotechnical engineering, sedimentology, glciology, landmine and UXO detection and classification, archaeology, etc, (see, e.g., [4]). Quantitative imaging needs to be performed in order to provide the high contrast and space resolution of marine CSEM or GPR sounding. In turn, quantitative imaging requires solving the Coefficient Inverse Problems (CIPs), i.e., the inverse problems for the partial differential equations where one needs to determine one or several coefficients from a given solution (or its functionals) on some manifolds (see, e.g., [6] and references cited there). Due to both the nonlinearity and ill-posedness of CIPs, providing the global convergence is very important for many, if not for all, reconstruction algorithms. Being applied to a CIP, the traditional nonlinear least squares approach normally results in a non-convex minimization problem. As a result, the traditional numerical techniques, such as the gradient or Newton-like methods, may not be applicable or they may fail to converge to the true solution or even to its estimates. On the other hand, the methods of global optimization are extremely time consuming and heuristic. The paper addresses a challenging problem of constructing computationally efficient algorithms for some CIPs arising in GPR and marine CSEM sounding.

One approach to constructing the computational algorithms for CIPs, the so-called convexification, was recently proposed in [6]. It is based on Carleman estimates allowing for constructing some strictly convex least squares functionals at each step of a layer stripping procedure with respect to the spatial variable. In [5] the layer stripping procedure with respect to the real-valued parameter of the Laplace transform combined with an iterative procedure for treatment of the so-called tails was developed and applied to solving nD ($n = 1, 2, 3$) CIPs. Unlike the numerical techniques described in [5], we do not solve an overdetermined boundary value problem when determining the initial approximations. Also, we do not use the marching scheme for performing iterates with respect to the parameter of the Laplace transform. Instead of the WKB (i.e., short wave) approximations, we use the true solution for a homogeneous medium in order to initialize the iterative procedure. The main distinctive feature of the proposed algorithm is minimizing the Tikhonov functional in the l_1-norm by Bregman iterations (see, e.g., [10]) or alternating direction method of multipliers (see, e.g., [3]) in combination with the refinement procedure, in which we search for a better approximation performing matching the interior field generated by the iterative solution by the solutions of the forward problem in the region of interest. It follows from the results of numerical experiments that these novelties are advantageous.

The paper is organized as follows. In the next section, we formulate the forward and inverse models. In the Section 3 we describe the proposed algorithm. In the Section 4 we show some results of numerical experiments with these models. We conclude the paper in Section 5.

2. THE FORWARD AND INVERSE MODELS

Without loss of generality and for the sake of clarity, consider a simple forward model of propagation and scattering of an electromagnetic pulse emitted at $z = 0$ and propagated through the

Epstein layer filled with the lossless inhomogeneous medium (see [9]). In this case, the Maxwell's equations together with the initial and boundary conditions can be reduced to the initial boundary value problem for the hyperbolic equation with respect to one of the electric components of the electromagnetic field

$$c^{-2}(z)(z)U_{tt} - U_{zz} = 0 \quad z > 0, t > 0, \tag{1}$$

$$U(z,0) = U_t(z,0) = 0, \ U(0,t) = \delta(t). \tag{2}$$

Here, $c(z)$ is the speed of propagation of electromagnetic waves. Note that the smallness assumption on the coefficient $c(z)$ is not imposed. This model may be suitable, for example, for quantitative imaging of the electric permittivity from the GPR data in regions with the arid climate. In conductive media, such as marine environments, the Equation (1) needs to be replaced with the parabolic equation. The inverse problem is formulated as follows. Given the function $U_z(0,t) = f(t)$, $t > 0$ and parameters $c_0 > 0, L > 0$, such that $c(z) = c_0$ for $z \geq L$, find the variable speed $c(z)$ on $(0, L)$.

Traditionally, the inverse model can be obtained by reducing the wave Equation (1) to the Helmholtz equation via the Fourier transform (see, e.g., [1]), [6, 8]). Unlike this model, we apply the Laplace transform

$$u(x,\nu) = \int_0^\infty U(z,t) \exp(-\nu t) dt, \ z > 0, \ \nu > \nu_0$$

to the problem (1)–(2) in accordance with [9]. Note that the Laplace transform needs to be slightly modified (e.g., by introducing $\exp(-\nu^2 t)$) for the parabolic problem. Introducing the dimensionless variables, we then obtain the s-parametric family of elliptic boundary value problems

$$u_{xx}(x,s) - s^2 n^2(x) u(x,s) = 0, \quad x \in (0,1), \quad s > s_0, \tag{3}$$

$$u(0,s) = 1, \tag{4}$$

$$u_x(1,s) + s u(1,s) = 0. \tag{5}$$

Here, $n(x) = c_0/c(x)$ is the refraction coefficient, $s_0(s) = \nu_0 L/c_0$, and $c(x)$ and c_0 are speeds of the wave propagation in the Epstein layer and homogeneous medium. Note that for a sufficiently smooth refraction coefficient $u(x,s) > 0$ (see, e.g., [6]).

In practice, the surface admittance $Y(s) = -u_x(0,s)/u(0,s)$ (or impedance) is measured in the interval $[\underline{s}, \overline{s}], \underline{s} > s_0$. Therefore, introducing by analogy with [6] the new function

$$v(x,s) = \frac{1}{s^2} \ln u, \tag{6}$$

we obtain the family of problems

$$v_{xx} + s^2 v_x^2 = n^2(x) \ \text{ in } (0,1), \quad s \in [\underline{s}, \overline{s}], \tag{7}$$

$$v(0,s) = 0, \quad v_x(1,s) = -\frac{1}{s}. \tag{8}$$

Introducing one more function $q(x,s) = \partial_s v(x,s)$ and differentiating (7), (8) with respect to the s-variable, we obtain the family of problems that do not contain the unknown refraction coefficient $n(x)$

$$q_{xx} + 2s^2 q_x v_x = -2s v_x^2 \ \text{ in } (0,1), \ s \in [\underline{s}, \overline{s}], \tag{9}$$

$$q(0,s) = 0, \quad q_x(1,s) = \frac{1}{s^2}. \tag{10}$$

Note that for every $s \in [\underline{s}, \overline{s}]$ the Equation (9) is integro-differential because of the representation

$$v(x,s) = -\int_s^{\overline{s}} q(x,\mu) d\mu + v(x,\overline{s}). \tag{11}$$

Thus, the inverse problem of frequency sounding is reduced, basically, to estimating the interior field $q(x,s)$ given the data $q_x(0,s) = (2Y(s)/s - Y'(s))/s^2 \equiv \Psi(s)$. Once such an estimate is obtained, the functions $v(x,s)$ and $n(x)$may also be estimated from (11) and (7).

3. THE ITERATIVE ALGORITHM

Initialization. The true solution of (7)–(8) for $n(x) \equiv 1$, i.e., the function is taken as the initial approximation

$$v^{(0)}(x,s) = -\frac{x}{s},$$

is taken as the initial approximation. Clearly, the corresponding function $q^{(0)}(x,s) = \frac{x}{s^2}$ is the true solution of the problem (9)–(10). Beginning with $v^0(x,s)$, we start the iterative process.

Step 1. Assume that the kth successive approximation $v^{(k)}(x,s)$ has been determined. Then, given $v^{(k)}(x,s)$, we determine $q^{(k)}(x,s)$ for every $s \in [\underline{s}, \overline{s})$ as follows. We approximate the second order ODE (9) together with the boundary conditions (10) and the data $Psi(s)$ by its finite-difference analogue, i.e., the system of linear equations $Ax = y$, and minimize the Tikhonov functional

$$T_\alpha[x] = \frac{1}{2}\|Ax - y\|_2^2 + \alpha R(x), \tag{12}$$

where $\alpha > 0$ is the regularization parameter. The stabilizing term $R(x)$ is chosen as either the l_1-norm $\|x\|_1$ or the total variation norm $\|x\|_{TV}$. Because of no strict convexity and differentiability, the alternating direction method of multipliers [3] or split Bregman algorithm [10] are applied to determine the minimizing sequences converging to the approximate solution $q^{(k+1)}(x,s)$.

Step 2. We update the function $v(x,s)$ for every parameter $s \in [\underline{s}, \overline{s})$ as follows.

$$v^{(k+1)}(x,s) = -\int_s^{\overline{s}} q^{(k+1)}(x,\nu)d\nu + v^{(k)}(x,\overline{s}), \tag{13}$$

$$v_x^{(k+1)}(x,s) = -\int_s^{\overline{s}} q_x^{(k+1)}(x,\nu)d\nu + v_x^{(k)}(x,\overline{s}), \tag{14}$$

$$v_{xx}^{(k+1)}(x,s) = -\int_s^{\overline{s}} q_{xx}^{(k+1)}(x,\nu)d\nu + v_{xx}^{(k)}(x,\overline{s}). \tag{15}$$

Step 3. Let $s^* \in [\underline{s}, \overline{s})$ be a certain number that does not depend on k. We update the refraction coefficient as

$$n_{k+1}^2(x) = v_{xx}^{(k+1)}(x,s^*) + s^2(v_x^{(k+1)}(x,s^*))^2, \tag{16}$$

where $x \in (0,1)$, and set $n_{k+1}(x) = 1$ for $x = 0$ and $x = 1$.

Step 4. Update the function $v(x,\overline{s})$ by first solving the problem

$$u_{xx}^{(k+1)}(x,\overline{s}) - \overline{s}^2 n_{k+1}^2(x) u(x,\overline{s}) = 0, \quad x \in (0,1), \tag{17}$$

$$u^{(k+1)}(0,s) = 1, \quad u_x^{(k+1)}(1,s) + s u^{(k+1)}(1,s) = 0. \tag{18}$$

and then determining the functions

$$v^{(k+1)}(x,\overline{s}) = \frac{\ln u^{(k+1)}(x,\overline{s})}{\overline{s}^2}, \tag{19}$$

$$v_x^{(k+1)}(x,\overline{s}) = \frac{u_x^{(k+1)}(x,\overline{s})}{\overline{s}^2 u^{(k+1)}(x,\overline{s})}, \tag{20}$$

$$v_{xx}^{(k+1)}(x,\overline{s}) = \frac{u_{xx}^{(k+1)}(x,\overline{s})}{\overline{s}^2 u^{(k+1)}(x,\overline{s})} - \left(\frac{u_x^{(k+1)}(x,\overline{s})}{\overline{s} u^{(k+1)}(x,\overline{s})}\right)^2 \tag{21}$$

for $x \in [0,1]$.

Stopping rule. If the level of noise δ in the data $\tilde{\Psi(s)}$ is given or it can be estimated, then it is natural to stop the process at the iterate $k_{stop} = \min\left\{k : \|\partial_x u_{n_k}(0,s) - \tilde{\Psi}(s)\|_{L_2[\underline{s},\overline{s}]} \le \delta\right\}$, where the function $u_n(x,s)$ is determined from the solution of the original problem (1)-(2) with $n(x) = n_k(x)$ for every successive approximation $n_k(x)$.

If the approximation $n_{k_{stop}}(x)$ does not possess high spatial and contrast resolutions then one may try to refine the pair $(\tilde{n}(x), \tilde{u}(x,s))$, where $\tilde{n}(x) = n_{k_{stop}}(x) \in G$ and $\tilde{u}(x,s) = \exp\left[s^2 v^{(k_{stop})}(x,s)\right]$. Note that although for a certain $s_* \in [\underline{s}, \overline{s})$ the function $\tilde{u}(x,s_*)$ may be close to the Laplace transform of the solution of the original problem (1)–(2), it does not satisfy it. This observation motivates matching the interior field $\tilde{u}(x,s_*)$ with the Laplace transform $u(x,s_*;n(x))$ of the solution of the original problem (1)–(2). We are interested in finding a new approximation of the true refraction coefficient $n^*(x)$ whose error estimate is better than the error estimate for $\tilde{n}(x)$. To find such an approximation, we consider the injective and continuous map $F(n) : n(x) \to u(x,s_*;n)$ and minimize the Tikhonov functional

$$T_\lambda[n] = \|F(n) - \tilde{u}(x,s_*;n)\|^2_{L_2(0,1)} + \lambda\|n - \tilde{n}\|_{L_1(0,1)}, \ \lambda > 0. \tag{22}$$

Let $n_\lambda(x)$ be the minimizer of the Tikhonov functional (22). By analogy with [7] one may conjecture that if the reqularization parameter is properly chosen, then

$$\left\|n_{\lambda(\gamma)} - n^*\right\| \leq \xi\|n^* - n_{k_{stop}}\|, \tag{23}$$

where $\xi \in (0,1)$. This motivates the refinement procedure.

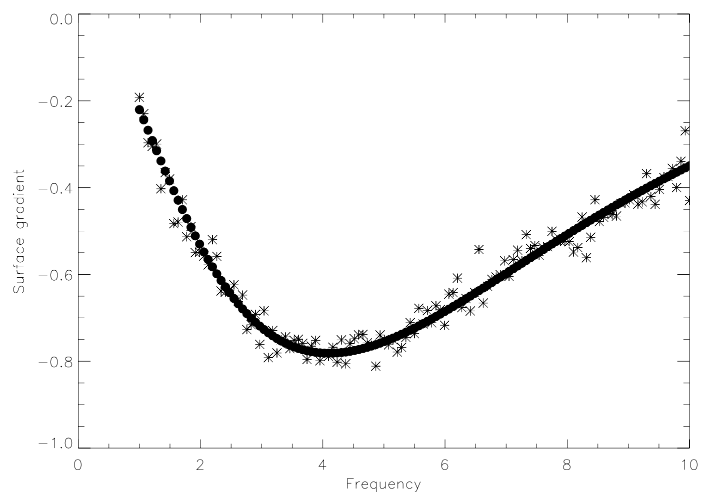

Figure 1: The simulated electromagnetic frequency data $\overline{\varphi}(s)$ in the interval $[1, 10]$. The noiseless data is shown by bullets and the data corrupted by noise at the level of 5% is shown by asterisks.

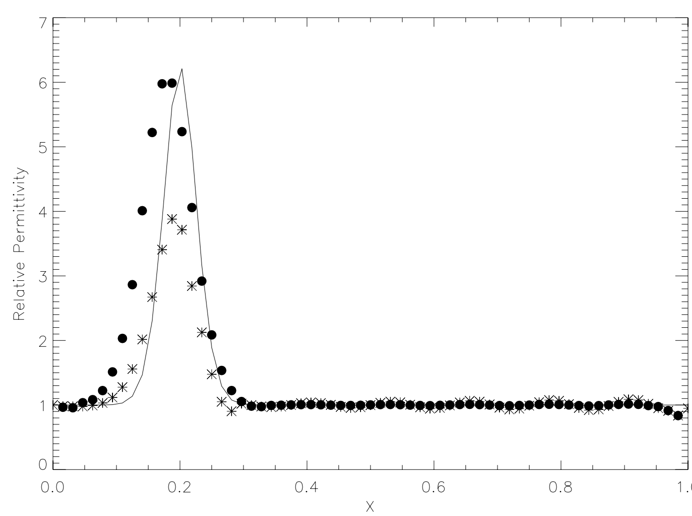

Figure 2: Recovering the relative electrical permittivity of a single mid-contrast land mine from the perturbed data (the level of noise is 5%) by the convexification method (asterisks) and proposed algorithm (bullets).

4. NUMERICAL EXPERIMENTS

To demonstrate the computational effectiveness of the proposed algorithm, we conducted several numerical experiments. As an example, we show the results reconstruction of the relative electrical permittivity of a subsurface land mine simulated by a Gaussian curve. To generate the frequency sounding data $\Psi(s)$, we solved numerically the problem (3)–(5). Figure 1 shows the typical perturbed boundary data generated by this mine embedded in the homogeneous background (air) with $\varepsilon = 1$. Figure 2 shows the mean relative electrical permittivity obtained from a sample containing twenty five realization of the pseudo-random vector.

5. CONCLUSIONS

In this paper, we briefly described the iterative algorithm for recovering the electrical permittivity or conductivity from the frequency sounding data. It was shown in numerical experiments that the proposed algorithm is capable of providing the high contrast and space resolution quantitative imaging. Future studies will be aimed at establishing the global convergence result, as well as at implementing the algorithm in high dimensions and conducting numerical experiments with the real data.

REFERENCES

1. Chen, Y. and V. Rokhlin, "On the inverse scattering problem for Helmholtz equation in one dimension," *Inverse Problem*, Vol. 8, 365–391, 1982.
2. Constable, S., "Ten years of marine CSEM for hydrocarbon exploration," *Geophysics*, Vol. 75, 75A67–75A81, 2010.
3. Eckstein, J. and D. Bertsekas, "On the Douglas-Rachford splitting method and the proximal point algorithm for maximal monotone operators," *Math. Programming*, Vol. 5, 293–381, 1992.
4. *Ground Penetrating Radar Theory and Applications*, Ed. by Jol, H. M., Elsevier, New York, 2009.
5. Kuzhuget, A. V., L. Beilina, M. V. Klibanov, et al., "Quantitative image recovery from measured blind backscattered data using a globally convergent inverse method," *IEEE Trans. Geoscience and Remote Sensing*, 1–12, 2012.
6. Klibanov, M. V. and A. Timonov, *Carleman Estimates for Coefficient Inverse Problems and Numerical Applications*, VSP, Utrecht, 2004.
7. Klibanov, M. V., A. B. Bakushinsky, and L. Beilina, "Why a minimizer of the Tikhonov functional is closer to the exact solution than the first guess," *J. Inv. Ill-Posed Problems*, Vol. 19, 83–105, 2011.
8. Sylvester, J., "Layer stripping," *Surveys on Solution Methods for Inverse Problems*, Ed. by Colton B, et al., Springer-Verlag, New York, 2000.
9. Tamasan, A. and A. Timonov, "On a new approach to frequency sounding of layered media," *Num. Func. Analysis and Optimization*, Vol. 29, 470–486, 2008.
10. Yang, Y., M. Moller, and S. Osher, "A dual split Bregman method for fast l^1 minimization," *Math. Comp.*, Vol. 82, 2061–2085, 2013.